Extraordinarily wide-view circular polarizers for liquid crystal displays

Zhibing Ge[1], Ruibo Lu[1], Thomas X. Wu[1], Shin-Tson Wu[1], Chao-Lien Lin[2], Nai-Chin Hsu[2], Wang-Yang Li[2], and Chung-Kuang Wei[2]

[1]College of Optics and Photonics, University of Central Florida, Orlando, Florida 32816, USA
[2]Chi Mei Optoelectronics, Tainan, Taiwan, 74144, R. O. C.

swu@mail.ucf.edu

Abstract: A new broadband wide-view circular polarizer is proposed for high transmittance multi-domain vertical-alignment liquid crystal displays (MVA LCDs). This configuration only requires one biaxial plate in the conventional circular polarizer. The optimal film parameters are obtained analytically through spherical trigonometric method on the Poincaré sphere and through computer-aided parameter search method. According to this design, the high transmittance MVA LCD exhibits a contrast ratio CR >200:1 over ~80° viewing cone.

OCIS codes: (230.3720) Liquid crystal devices; (260.5430) Polarization; (999.9999) Circular polarizer

References and links:

1. A. Takeda, S. Kataoka, T. Sasaki, H. Chida, H. Tsuda, K. Ohmuro, T. Sasabayashi, Y. Koike, K. Okamoto, "A super-high image quality multi-domain vertical alignment LCD by new rubbing-less technology," Soc. Inf. Display Tech. Digest **29**, 1077-1080 (1998).
2. R. A. Soref, "Field effects in nematic liquid crystals obtained with interdigital electrodes," J. Appl. Phys. **45**, 5466–5468 (1974).
3. M. Oh-e, M. Ohta, S. Aratani, and K. Kondo, "Principles and characteristics of electro-optical behavior with in-plane switching mode," Proc. 15th Int'l Display Research Conf., 577–580 (1995).
4. J. Chen, K. H. Kim, J. J. Jyu, J. H. Souk, J. R. Kelly, and P. J. Bos, "Optimum film compensation modes for TN and VA LCDs," Soc. Inf. Display Tech. Digest **29**, 315-318 (1998).
5. X. Zhu, Z. Ge, and S. T. Wu, "Analytical solutions for uniaxial-film-compensated wide-view liquid crystal displays," J. Display Technology **2**, 2-20 (2006).
6. Y. Iwamoto and Y. Iimura, "Transmittance enhancement for randomly aligned liquid crystal displays with circular polarizers," Jpn. J. Appl. Phys. **41**, L1383-L1385 (2002).
7. H. Yoshida, Y. Tasaka, Y. Tanaka, H. Sukenori, Y. Koike, and K. Okamoto, "MVA LCD for notebook or mobile PCs with high transmittance, high contrast ratio, and wide angle viewing," Soc. Inf. Display Tech. Digest **35**, 6-9 (2004).
8. H. Yoshimi, S. Yano, and Y. Fujimura, "Optical films for reflective LCDs to achieve high image quality," Soc. Inf. Display Tech. Digest **33**, 862-865 (2002).
9. Q. Hong, T. X. Wu, X. Zhu, R. Lu, and S. T. Wu, "Designs of wide-view and broadband circular polarizers," Opt. Express **13**, 8318-8331 (2005).
10. Q. Hong, T. X. Wu, R. Lu, and S. T. Wu, "Wide-view circular polarizer consisting of a linear polarizer and two biaxial films," Opt. Express **13**, 10777-10783 (2005).
11. H. Lin, "Extraordinarily wide-view and high-transmittance vertically aligned liquid crystal displays," Appl. Phys. Lett. **90**, 151112 (2007).
12. S. Huard, *Polarization of Light* (Wiley, New York, 1997).
13. A. Lien, "Extended Jones matrix representation for the twisted nematic liquid-crystal display at oblique incidence," Appl. Phys. Lett. **57**, 2767-2769 (1990).
14. Z. Ge, T. X. Wu, X. Zhu, and S. T. Wu, "Reflective liquid crystal displays with asymmetric incidence and exit angles," J. Opt. Soc. Am. A **22**, 966-977 (2005).
15. P. Yeh and C. Gu, *Optics of Liquid Crystal Displays* (Wiley, New York, 1999).
16. J. D. H. Donnay, *Spherical Trigonometry* (Church Press, 2007).
17. Y. Fujimura, T. Kamijo, and H. Yoshimi, "Improvement of optical films for high performance LCDs," Proc. SPIE **5003**, 96-105 (2003).
18. Z. Ge, T. X. Wu, R. Lu, X. Zhu, Q. Hong, and S. T. Wu, "Comprehensive three-dimensional dynamic modeling

of liquid crystal devices using finite element method," J. Display Technology **1**, 194-206 (2005).

19. X. Zhu, Z. Ge, T. X. Wu, and S. T. Wu, "Transflective liquid crystal displays," J. Display Technology **1**, 15-29 (2005).
20. M. P. Hong, S. I. Kim, Y. C. Yang, K. Chung, H. W. Do, S. J. Park, C. G. Jhun, G. D. Lee, T. H. Yoon, and J. C. Kim, "Low-twist vertically-aligned transflective LCD," Soc. Inf. Display Tech. Digest **35**, 34-37 (2004).
21. Z. Ge, X. Zhu, R. Lu, T. X. Wu, and S. T. Wu, "Transflective liquid crystal display using commonly biased reflectors," App. Phys. Lett. **90**, 221111 (2007).

1. Introduction

High contrast ratio and wide viewing angle are two critical requirements for liquid crystal displays (LCDs), such as LCD TVs, desktop monitors, and notebook computers. To achieve wide viewing angle, a good dark state over a large viewing cone must be maintained. Currently, multi-domain vertical-alignment (MVA) mode [1] and in-plane switching (IPS) mode [2, 3] are the two major approaches meeting these requirements. A MVA LCD exhibits an inherent high contrast ratio at normal incidence because the LC molecules are initially aligned vertically to the substrates. To minimize the light leakage at oblique angles, various phase compensation schemes under crossed linear polarizers have been developed [4, 5]. However, a shortcoming of a MVA LCD employing crossed linear polarizers is the reduced transmittance. Ideally, the LC directors should be all rotated 45° with respect to the polarizer's optic axis in order to achieve maximum transmittance in a voltage-on state. But in reality, the LC director's reorientation is not very uniform. As a result, the transmittance is decreased.

To enhance transmittance, a circularly polarized light is preferred because it is independent of the LC director's reorientation angle [6, 7]. A typical circular polarizer consists of a linear polarizer and a quarter-wave plate with its optic axis oriented at 45° from the polarizer's transmission axis. A MVA cell sandwiched between two crossed circular polarizers has a broad bandwidth in the visible spectral region (as the two quarter-wave plates from the bottom and top circular polarizers are crossed to each other to have a self-compensation for wavelength dispersion), but its viewing angle is too narrow. This is because the off-axis light leakage from the combination of LC layer (even if it is compensated by a negative C-plate), two quarter-wave plates, crossed linear polarizers cannot be eliminated at all angles. Recently, some wide-view and broadband circular polarizers have been proposed [8-11]. For instance, Hong et al designed a wide-view circular polarizer using a linear polarizer and two biaxial films [10]. This design significantly widens the acceptance angle, but the tradeoff is the increased cost. In Ref. 11, Lin proposed another circular polarizer configuration for MVA LCDs, where the two quarter-wave plates from two crossed circular polarizers consist of a positive A-plate and a negative A-plate. In his design, two opposite quarter-wave plates are aligned parallel to each other so that the self-compensation effect occurs regardless of the viewing direction. Besides, two more A-plates are also employed for the compensation of the crossed linear polarizers. This design greatly simplifies the device configuration while maintaining an excellent viewing angle, but two negative A-plates are required. All the abovementioned designs require one or more additional negative C-plates to fully cancel the phase retardation from the LC layer.

In this paper, we propose a new wide-view circular polarizer for MVA LCDs that only requires one additional biaxial plate from a conventional crossed circular polarizer. The device configuration is shown in Fig. 1. This design uses the least number of wave plates to achieve wide view. In our design, the negative C-plate is intended to partially compensate the phase retardation from the LC layer. After optimization, the residual phase retardation from the negative C-plate and LC layer (a positive C-plate) together with the biaxial plate can compensate for all incident angles. Besides, the required phase retardation value ($d\Delta n/\lambda$) of the effective positive C-plate can be analytically determined by a spherical trigonometric method on the Poincaré sphere [12]. The parameters of the biaxial plate are then obtained by computer optimization. To verify the proposed optical configuration, we calculated its performance in a 4-domain MVA structure. This simple design leads to an excellent dark state over the entire 90° viewing cone and a contrast ratio over 200:1 is expanded to ~80° viewing cone.
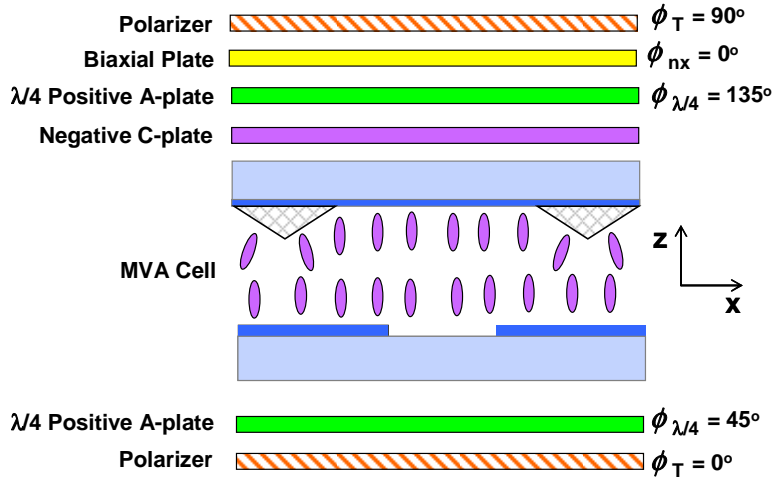
Fig. 1. Schematic of a MVA cell under the new circular polarizer with one biaxial film.

2. Design of wide-view circular polarizer for MVA cells

2.1. Light leakage from conventional circular polarizers

Before demonstrating our designs to achieve wide-viewing angle, we first studied the origins of off-axis light leakages from two crossed conventional circular polarizers (each consisting of a linear polarizer and a quarter-wave plate oriented at 45° from the polarizer's transmission axis). We traced the change of polarization state of the incident light through this system on the Poincaré sphere. The Stokes parameters related to each polarization state are obtained by solving the electric fields using the 2-by-2 matrix method [13, 14]. Here we plotted the polarization change of the incident light at two different azimuthal directions φ_{inc} = -45° and φ_{inc} = 0°, while the incident polar angle θ_{inc} is kept at 70° for both cases. At the beginning stage, the effects from the LC layer and negative C-film are excluded. Their effects will be included later.

The first factor that affects the viewing angle is the deviation of effective polarizer angle viewed at an oblique direction. At the bisector direction with φ_{inc} = -45° and θ_{inc}=70° as shown in Fig. 2(a), point **P** and point **A** on the equator represent the absorption axis of the bottom and top linear polarizer, respectively. As an opposite extent of **OP**, the point **T** on the other side of equator stands for the transmission axis of the bottom polarizer, i.e., the polarization state of the incident light passing the bottom linear polarizer. Here at this bisector direction with θ_{inc}=70°, point **T** and point **A** depart from each other, indicating a light leakage. This deviation can be depicted by $\angle TOA$ in the Poincaré sphere, which is the supplementary angle of $\angle POA$. Generally, for two axes aligned at φ_1 and φ_2 in the x-y plane, their effective angle $\delta_{2,1}$ in the media (with refractive index of n_p) for the incident light at an oblique direction (φ_{inc}, θ_{inc}) from the air can be expressed as [5]:

$$\delta_{2,1} = \cos^{-1}\left(\frac{\cos(\varphi_2 - \varphi_1) - (\sin^2\theta_{inc}/n_p^2)\cos(\varphi_1 - \varphi_{inc})\cos(\varphi_2 - \varphi_{inc})}{\sqrt{1 - (\sin^2\theta_{inc}/n_p^2)\cos^2(\varphi_1 - \varphi_{inc})}\sqrt{1 - (\sin^2\theta_{inc}/n_p^2)\cos^2(\varphi_2 - \varphi_{inc})}}\right) . \quad (1)$$

For the crossed polarizers considered here, φ_1=0°, φ_2=90°, and average polarizer refractive index n_p ~1.5. In addition, when represented on the Poincaré sphere, a factor of 2 needs to be included, leading to $\angle POA = 2\delta_{2,1}$ and $\angle TOA = \pi - 2\delta_{2,1}$. Thus, when φ_{inc} =-45° and θ_{inc}=70°, $\angle TOA$ is ~28.26^o, which is quite a large deviation from 0° at normal incidence.

A second factor degrading the viewing angle is the off-axis phase retardation from each uniaxial quarter-wave plate. The effective retardation value of the A-plate and C-plate can be described as follows [5, 15]:

$$\Gamma_a = \frac{2\pi}{\lambda} d \left[n_e \sqrt{1 - \frac{\sin^2(\varphi_n - \varphi_{inc})\sin^2\theta_{inc}}{n_e^2} - \frac{\cos^2(\varphi_n - \varphi_{inc})\sin^2\theta_{inc}}{n_o^2}} - n_o \sqrt{1 - \frac{\sin^2\theta_{inc}}{n_o^2}} \right]. \quad (2)$$

and

$$\Gamma_c = \frac{2\pi}{\lambda} d n_o \left[\sqrt{1 - \frac{\sin^2\theta_{inc}}{n_e^2}} - \sqrt{1 - \frac{\sin^2\theta_{inc}}{n_o^2}} \right], \quad (3)$$

where ϕ_n is the alignment angle of the optic axis of the A-plate, and n_e and n_o are the refractive index of the plate, respectively.

From Fig. 2(a), the incident light passing the bottom linear polarizer is first moved to point **B** by the bottom quarter-wave plate (this trace is a rotation of point **T** to point **B** along the $+S_1$ axis), and is further converted to point **F** by the subsequent top quarter-wave plate (which is a rotation along the $-S_1$ axis). For $\varphi_{inc}=-45^o$, the retardation value for the bottom quarter-wave plate (with $\phi_n=45^o$) is larger than that from the top quarter-wave plate (with $\phi_n=135^o$), as indicated from Eq. (2) and is verified in Fig. 2(a) from simulation. The shorter trace **BF** with respect to trace **TB** on the Poincaré sphere makes final point **F** deviated even more from the absorption axis of the top linear polarizer at point **A**.
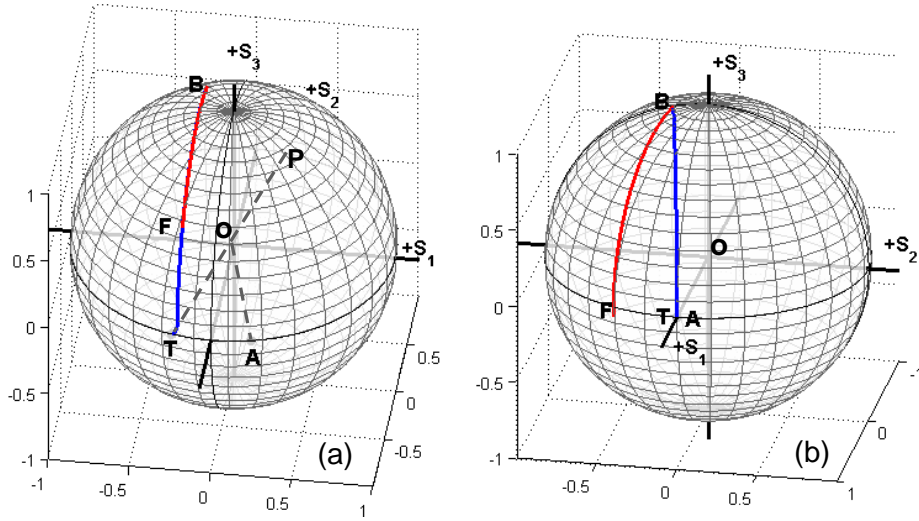

Fig. 2. Polarization state trace on the Poincaré sphere at $\theta_{inc} = 70°$, (a) $\varphi_{inc} = -45°$ and (b) $\varphi_{inc} = 0°$.

On the other hand, when viewed at $\varphi_{inc}=0^o$ and $\theta_{inc}=70^o$, the transmission axis of the bottom polarizer at point **T** overlaps with the absorption axis of the top polarizer at point **A**, as their effective angle $\delta_{2,1}$ from Eq. (1) is always equal to 90° independent of the polar angle θ_{inc}. However, based on Eq. (1) the optic axes of the two quarter-wave plates viewed at $\varphi_{inc} = 0^o$ and $\theta_{inc}=70^o$ are no longer $\pm45^o$ from the polarizer's transmission axis. Hence, their corresponding effective optic axes on the Poincaré sphere are no longer parallel to each other, making the rotational trace **BF** and trace **TB** separated, as shown in Fig. 2(b).

Figure 3 plots the light leakage from above two crossed circular polarizers viewed from different directions. As we can see, the 10% light leakage (~0.034) occurs at about 60° and the

global maximum value is about 0.04, which is inadequate for achieving a high contrast ratio at wide angles.
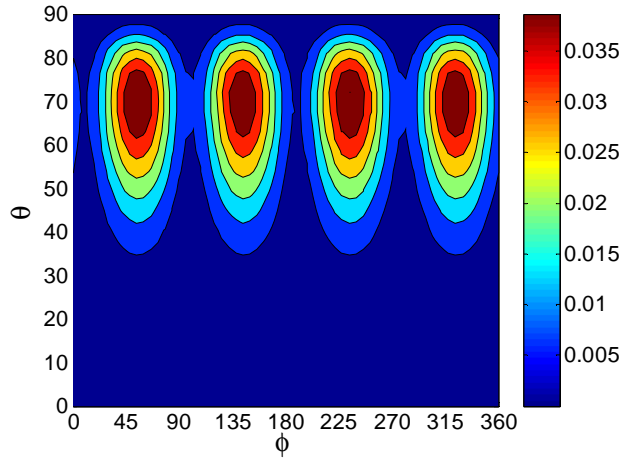

Fig. 3. Angular light leakage from two crossed circular polarizers each consisting of a linear polarizer and a quarter-wave plate, and the maximum transmittance from two parallel linear polarizers is ~34%.

2.2. Determination of phase retardation for the effective positive C-plate

In our circular polarizer configuration shown in Fig. 1, we intentionally design the negative C-plate to partially compensate the LC layer (a positive C-plate), making them together perform like a positive C-plate. This additional effective positive C-plate yields a complete compensation for $\varphi_{inc} = 0^o$ and $\theta_{inc}=70^o$. Along with this C-plate, the biaxial plate works to compensate the other direction at $\varphi_{inc} = -45^o$ and $\theta_{inc}=70^o$.
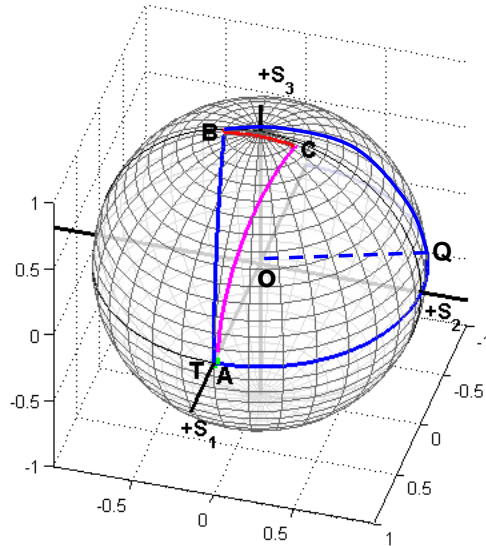

Fig. 4. Spherical angle relations on the Poincaré sphere at $\varphi_{inc} = 0^o$ and $\theta_{inc}=70^o$.

Figure 4 shows the polarization trace on the Poincaré sphere when viewed at $\varphi_{inc} = 0^o$ and $\theta_{inc}=70^o$, after inserting an effective positive C-plate between the two crossed quarter-wave plates. Here, the bottom quarter-wave plate converts the light from point **T** to point **B** as before.

Then, the effective positive C-plate functions to move the light from point **B** to point **C**, where the subsequent top quarter-wave plate can transfer the light from point **C** completely to the absorption direction at point **A** of the top polarizer, rather than that in Fig. 2(b). In addition, under such a condition, point **B** and point **C** are symmetric along the S_1-S_3 plane.

The required phase retardation of the effective positive C-plate can be analytically derived by a spherical trigonometric method on the Poincaré sphere. The first bottom quarter-wave plate rotates the light polarization from point **T** to point **B** along its effective optic axis **OQ** on the Poincaré sphere, as shown in Fig. 4. Then the effective positive C-plate rotates the polarization from point **B** along the $+S_1$ axis, therefore the rotational spherical angle $\angle BTC$ is equal to the related retardation of the C-plate. Here because of the symmetry between the spherical arc $\overline{TB}$ and arc $\overline{AC}$ (please note here the polarization trace **TB** (or **AC**) is not equivalent to the described spherical arc $\overline{TB}$ (or $\overline{AC}$), which must be defined on the large circle on a sphere), spherical angle $\angle BTC = \pi - 2\angle CAQ = 2\angle BTQ - \pi$. And the spherical angle $\angle BTQ$ can be calculated from the geometric relations in the spherical triangle **BTQ**, where spherical arcs $\overline{TQ}$, $\overline{BQ}$, and spherical angle $\angle BQT$ can be uniquely determined by the polarization rotation from the bottom quarter-wave plate. In spherical triangle **BTQ**, arc $\overline{TQ}$ is equal to arc $\overline{BQ}$, which further equals to the $\angle TOQ$ (assuming the radius of this sphere is 1). From Eq. (1) by setting $\varphi_1 = 0^o$ and $\varphi_2 = 45^o$, and $n_{e\_A} = 1.5902$, $n_{o\_A} = 1.5866$ (at $\lambda = 550$ nm) (here $n_p \sim 1.58$), we can obtain $\angle TOQ = 2\delta_{2,1} \sim 102.4^o$, yielding arc length $\overline{TQ} = \overline{BQ} \sim 1.787$. Besides, the spherical angle $\angle BQT$ is equal to the off-axis phase retardation of the uniaxial quarter-wave A-plate that can be obtained from Eq. (2) [5]. Using positive A-plate parameters with alignment angle $\phi_n = 45^o$, the spherical angle $\angle BQT$ is $\sim 92.08^o$. From the spherical trigonometry, in spherical triangle **BTQ**, we can first calculate the spherical arc $\overline{TB}$ (please notice the polarization trace **TB** on the sphere is not equivalent to the spherical arc $\overline{TB}$) to get spherical angle $\angle BTQ$ from the following equation [16]

$$\overline{TB} = \cos^{-1}(\cos^2(\overline{TQ}) + \sin^2(\overline{TQ})\cos(\angle BQT)), \tag{4}$$

and

$$\angle BTQ = 2\cos^{-1}(\sqrt{\sin(s)\sin(s - \overline{BQ})/\sin(\overline{TB})/\sin(\overline{TQ})}), \tag{5}$$

where $s = \frac{1}{2}(\overline{TQ} + \overline{TB} + \overline{BQ})$. From these relations, we find arc $\overline{TB}$ ~ 1.5592 and $\angle BTQ \sim 102.56^o$. Hence, the spherical angle $\angle BTC = 2\angle BTQ - \pi$ is $\sim 25.12^o$, which is also equal to the retardation of the effective positive C-plate as described in Eq. (3).

Therefore, if the refractive indices n_{e_C} and n_{o_C} for the effective positive C-plate are also set as 1.5902 and 1.5866, we find the preferred dΔn/λ value of the C-plate is about 0.16. Besides, we find this retardation almost maintains a constant value over a wide range of θ_{inc} that changes from 1° to 89°, as plotted in Fig. 5. This means we can set the retardation value for the required effective positive C-plate that comes from the partial compensation between the negative C-plate and the LC cell at one oblique angle and it will work equally well for all other incident polar angles.

Furthermore, the light at point **C** after the effective positive C-plate is converted to point **A** by the top quarter-wave plate. Here because we align the n_x axis of the biaxial plate along the bottom polarizer transmission axis, the light at point **A** maintains its polarization passing the biaxial plate, thus is fully absorbed by the top linear polarizer.
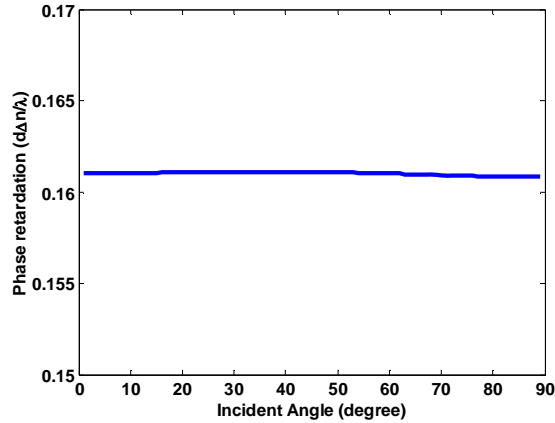
Fig. 5. Phase retardation of the effective positive C-plate with different incident angle θ_{inc} at φ_{inc} = 0°.

2. 3. Determination of biaxial plate in the circular polarizers

At other incident direction with φ_{inc} = -45° and θ_{inc}=70°, the bottom polarizer transmission axis at point **T** deviates from the top polarizer absorption direction at point **A**, as shown in Fig. 6. The first quarter-wave plate transfers the incident light from the bottom polarizer to point **B**, then the following effective positive C-plate moves it further to point **C** along the -S_1 axis. After that, the top quarter-wave plate further converts the light to point **D**. At this direction with φ_{inc} = -45° and θ_{inc}=70°, the biaxial plate works on the impinging light polarization change. For a biaxial plate, it can be characterized by its N_z factor ($N_Z = (n_x - n_z)/(n_x - n_y)$) and its in-plane phase retardation $d(n_x-n_y)/\lambda$ [17]. By properly tuning these two parameters while plotting the polarization trace on the Poincaré sphere, we find when $N_z \sim 0.35$ and $d(n_x-n_y)/\lambda \sim 0.34$ the final polarization after the biaxial plate can reach the top linear polarizer's absorption axis at point **A**, i.e., the light leakage is minimized. The calculated polarization trace from simulation is shown in Fig. 6.
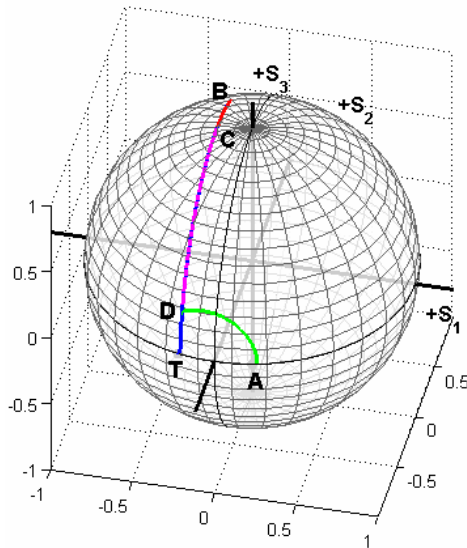

Fig. 6. Polarization trace on the Poincaré sphere at φ_{inc} = -45° and θ_{inc}=70°.

3. Results and Discussion

We applied the abovementioned optical configuration to a 4-domain MVA cell with cell gap d=4 μm. The LC material employed is Merck MLC-6608; its parameters are listed below: extraordinary and ordinary refractive indices $n_e = 1.5578$, $n_o = 1.4748$ (at λ=589 nm), parallel and perpendicular dielectric constants $\varepsilon_{//} = 3.6$, $\varepsilon_{\perp} = 7.8$, and elastic constants $K_{11} = 16.7$ pN and $K_{33} = 18.1$ pN. The negative C-plate used here has extraordinary and ordinary refractive indices $n_e = 1.5024$ and $n_o = 1.4925$ (at λ=550 nm). We calculated the LC directors distribution by the finite element method [18], and the corresponding optical properties, e.g., angular light leakage and viewing angle, by the 2x2 matrix methods [13, 14]. During calculations, we found when the overall phase retardation of the effective positive C-plate (that comes from the partial compensation of the LC layer by the negative C-plate) is about 0.17, a globally minimized light leakage was obtained. This value is very close to 0.16, the value we derived analytically.

Figure 7 shows the simulated brightness distribution of the 4-domain MVA cell under linear polarizers (top) and proposed circular polarizers (bottom). Because the LC directors do not tilt towards the preferred directions that are ±45° with respect to the polarizer transmission axis near the chevron-shaped slit regions, the output transmittance under two crossed linear polarizers is only about 23.0%. For comparison, the maximum transmittance T_{max} from two parallel polarizers employed here is about 34%. However, under circular polarizers, as its dependence of the rotation angle φ is removed, the transmittance is increased to ~30.4% and is much more uniform. Thus, the proposed circular polarizers have enhanced the brightness of the MVA cell by ~30%, which is beneficial for reducing power consumption.
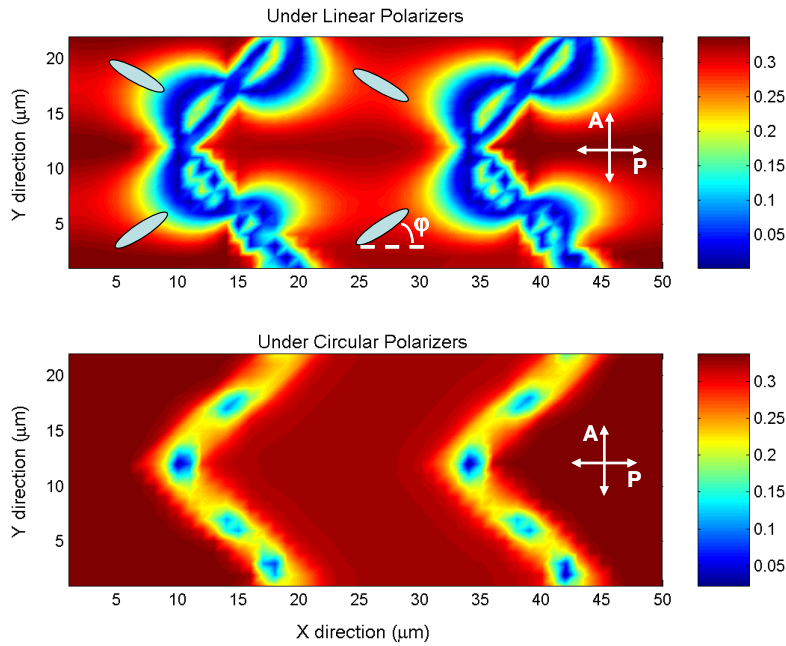

Fig. 7. Transmittance for a 4-domain MVA cell under crossed linear polarizers (top) and proposed circular polarizers (bottom) at normal incidence and λ=550 nm.

In addition to the enhanced transmittance, the off-axis light leakage of the MVA cell using our new circular polarizers is also suppressed significantly. Figure 8(a) shows the angular light leakage with a global maximum value below 5×10^{-4}. Accordingly, the corresponding viewing angle of this display as plotted in Fig. 8(b) is also greatly widened. The contrast ratio >200:1 over ~80° viewing cone is obtained.
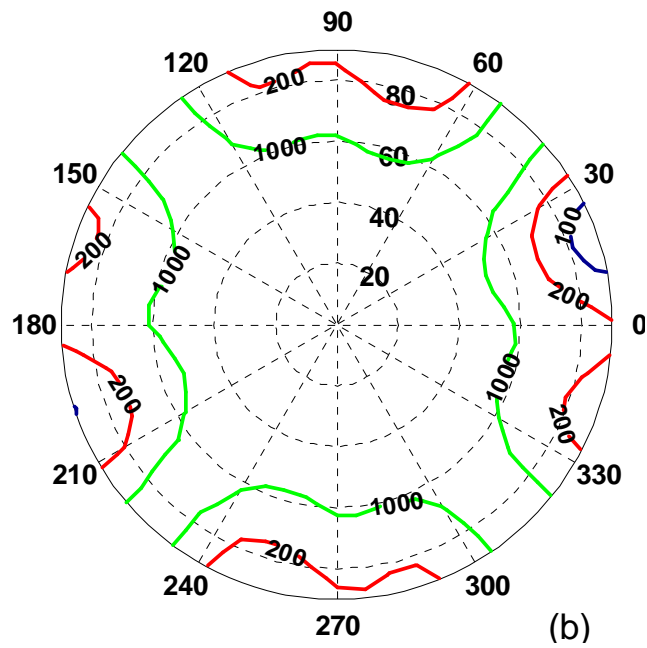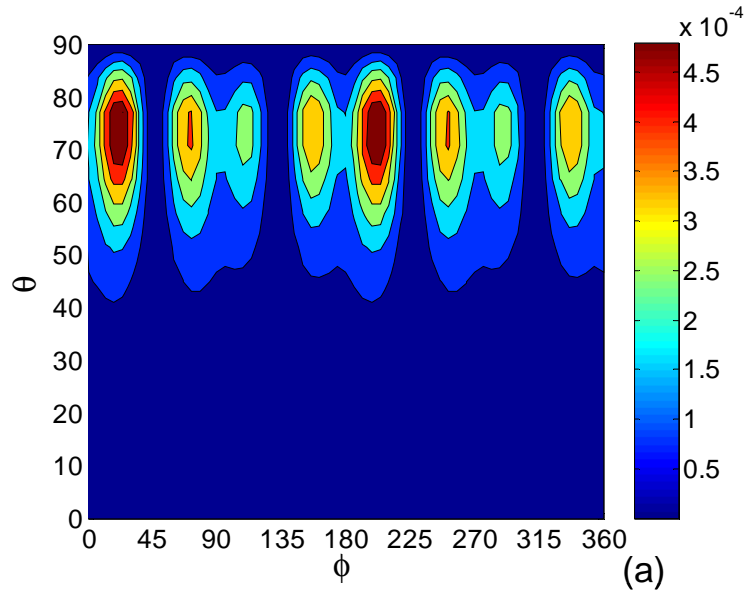
Fig. 8. (a) Angular light leakage of the MVA using this new circular polarizer and (b) its iso-contrast plot at λ= 550 nm.

In comparison to linear polarizers, our circular polarizers have similar performances in terms of viewing angle, light leakage, and spectral bandwidth, but have a ~30% higher transmittance for a 4-domain MVA-LCD. In comparison to conventional circular polarizers, our circular polarizers exhibit a similar broad bandwidth, but much wider viewing angle and higher contrast ratio. As a result, our new circular polarizers can also be used in transflective LCDs, where the reflective mode usually requires a top circular polarizer in order to achieve a good dark state [19-21]. By using these new circular polarizers in a transflective LCD, we can also obtain both wide view angle and high contrast ratio.

4. Conclusion

We demonstrated a new wide-view circular polarizer for high transmittance MVA LCDs. This wide-view design only introduces a single biaxial plate into the conventional circular polarizer configuration for MVA LCDs, where the partial compensation between the negative C-plate and the LC layer, along with the biaxial plate significantly suppressed the off-axis light leakage in omni directions. The related methodology for retardation plate design is also discussed in detail. We believe these circular polarizers will make important impact to the next generation wide-view and high transmittance MVA LCDs in both transmissive and transflective displays.

Acknowledgments